Determination of γ/γ' interface free energy for solid state precipitation in Ni-Al alloys from molecular dynamics simulation **②**

Jacob P. Tavenner ■ [0]; Mikhail I. Mendelev [0]; Raymond Neuberger [0]; Raymundo Arroyave [0]; Richard Otis; John W. Lawson



J. Chem. Phys. 161, 041102 (2024) https://doi.org/10.1063/5.0217993









18 September 2024 19:45:19



Determination of γ/γ' interface free energy for solid state precipitation in Ni-Al alloys from molecular dynamics simulation

Cite as: J. Chem. Phys. 161, 041102 (2024); doi: 10.1063/5.0217993

Submitted: 8 May 2024 • Accepted: 8 July 2024 •

Published Online: 23 July 2024







Jacob P. Tavenner, 1,a) D Mikhail I. Mendelev, 2,b) Raymond Neuberger, 3 D Raymundo Arroyave, 3 D

Richard Otis.4 and John W. Lawson2





AFFILIATIONS

- KBR, Inc., Intelligent Systems Division, NASA Ames Research Center, Moffett Field, California 94035, USA
- ²Intelligent Systems Division, NASA Ames Research Center, Moffett Field, California 94035, USA
- 3 Department of Materials Science and Engineering, Texas A & M University, College Station, Texas 77843, USA
- Engineering and Science Directorate, Jet Propulsion Laboratory, California Institute of Technology, Pasadena, California 91011, USA

b) mikhail.mendelev@nasa.gov

ABSTRACT

Interface free energy is a fundamental material parameter needed to predict the nucleation and growth of new phases. The high cost of experimentally determining this parameter makes it an ideal target for calculation through a physically informed simulation. Direct determination of interface free energy has many challenges, especially for solid-solid transformations. Indirect determination of the interface free energy from the nucleation data has been done in the case of solidification. However, a slow on molecular dynamics (MD) simulation time scale atomic diffusion makes this method not applicable to the case of nucleation from the solid phase when precipitate composition is different from that in matrix. To address this challenge, we outline the development of a new technique for determining the critical nucleus size from an MD simulation using a recently developed method to accelerate solid-state diffusion. The accuracy of our approach for the Ni-Al system for Ni₃Al (γ') precipitates in a Ni-Al (γ) matrix is demonstrated well within experimental accuracy and greatly improves upon previous computational methods [Herrnring et al., Acta Mater. 215(8), 117053 (2021)].

Published under an exclusive license by AIP Publishing. https://doi.org/10.1063/5.0217993

I. INTRODUCTION

The precipitation of a second phase can significantly affect a wide variety of material properties, including mechanical to optical, electrical, and beyond. Precise heat treatments can be used to produce materials with finely tuned and optimized properties for nearly any task. In practice, however, heat treatments for precipitation are often not used to their full potential because of the inherent difficulty in accurately predicting a precipitation response, often requiring expensive experimentation and trial/error to design treatments. While a variety of methods exist to predict and model the precipitation behavior, such as phase-field and Kampmann-Wagner Numerical (KWN) modeling, the practical application of these methods to heat treatment design is severely hindered by their

extreme dependence on the interface free energy between the precipitate and its parent phase, a value that is notoriously difficult to measure experimentally. KWN modeling, for example, is based on the classical nucleation theory (CNT), where the equation for nucleation rate contains a cubic interface free energy term inside of an exponential function. Due to the nature of precipitation reactions, any variation in nucleation rate compounds over the course of the heat treatment, meaning that even minute differences in the interface free energy value can cause many orders of magnitude differences in the number of predicted particles.

Considering the enormous difficulty of direct measuring the interface free energy experimentally, atomistic computer simulation is an attractive alternative method of obtaining this quantity. Two points should be immediately made: First, the interface free energy

a) Author to whom correspondence should be addressed: jacob.p.tavenner@nasa.gov

depends on temperature, and, therefore, the calculations should be performed at the temperature of interest. Second, the interface profile fluctuates at any finite temperature and these inherent fluctuations cannot be ignored, as they contribute significantly to the interfacial free energy.²⁻⁴ These two points efficiently rule out the possibility of determining interface free energy using the T = 0 small simulation cells typical in ab initio calculations, necessitating instead larger scale molecular dynamics (MD) or Monte Carlo (MC) atomistic simulations. Therefore, employing a classical semiempirical potential or a machine learning (ML) potential is required. Such potentials have been developed for decades, and the best of them are capable of accurately reproducing mechanical and defect properties. In the case of simulating an interface between two phases, the main requirement is a good reproduction of chemical partitioning behavior, which is almost never included in the potential development procedure. This can be a serious problem for the determination of the interface energy.

There are several ways of determining the interface free energy through atomistic simulations. In the cleaving method proposed in Refs. 5 and 6, this is accomplished by determining the reversible work required to transform separate bulk simulation cells containing one of the co-existing phases into a single simulation cell containing both phases and the interface. In the capillarity fluctuation method (CFM) proposed in Ref. 2, the interface free energy is determined from the analysis of fluctuations of the interface profile. Finally, the interface free energy can be determined using the seeding method from the critical nucleus size employing classical nucleation theory. 7-10 All these approaches were primarily developed for solid-liquid interfaces, and application to solid-solid interfaces has been limited. In most cases, a newly growing phase has a composition different from that of the parent phase, and, therefore, the growth is controlled by atomic diffusion. In the case of solid-liquid interfaces, this diffusion proceeds in a liquid phase and is fast enough to be captured in an MD simulation. Atomic diffusion in crystal phases is much slower than that in liquids and can be barely observed during an MD simulation, which prevents obtaining any reasonable statistics about the interface properties.

The recently developed MD-based kinetic Monte Carlo approach¹¹ (referred below as kMC/MD) enables simulations to overcome the slow diffusion problem. In this approach, the MD simulation used to model atomic motion is interrupted to perform MC swaps. The difference between this method and the more conventional MC/MD method implemented in the LAMMPS (Large-scale Atomic/Molecular Massively Parallel Simulator) package¹² is that the swaps in the kMC/MD approach¹¹ are allowed only with neighbor atoms, which are automatically determined using the Voronoi tessellation. This nearest-neighbor sampling restricts the available sampled ensemble to only include states that are kinetically available to the system through a physically based diffusion pathway. For example, suppose that a precipitate has a large second element concentration than does the matrix and the interface advances toward the matrix. Then, the matrix at this point should be depleted by the second element. In the case of standard MC/MD, the second element concentration can be easily restored because atoms can be taken from any place in the simulation cell. In the case of kMC/MD, the second element atoms can come only from the vicinity of this point making such fluctuation less probably. Therefore, the interface profile fluctuations will be higher in the case of standard MC/MD, which

will translate into an underestimated value of the interface stiffness and interface energy itself.²

While in principle the kMC/MD method can be formulated to mimic the real kinetics of a process under consideration, this is not necessary to get an equilibrium property such as interface free energy. Therefore, it can be used in combination with any of the three methods to obtain the interface free energy mentioned above. In the present study, the seeding method was selected.

This new kMC/MD hybrid simulation technique was applied to study precipitation of the L_{12} Ni₃Al compound (γ' phase) from a Ni-based fcc solution (y phase). This choice of system was motivated by two factors. First, a semiempirical potential employed in the determination of the interface free energy should correctly reproduce the alloy element partitioning. Recently, we have developed a Ni-Al Finnis-Sinclair¹³ (FS) type interatomic potential for the Nirich part of the Ni-Al phase diagram. 14 This potential provides very good agreement with experimental data for the element partitioning between the γ and γ' phases. Second, our choice was motivated by the fact that the Ni-based superalloys are widely used as creep resistant materials for high temperature applications. Therefore, the Ni-Al system, which is the basis for these alloys, has been intensively studied, and there are experimental data on the $\gamma-\gamma'$ interface free energy. These data were used in the present study to evaluate the reliability of the simulation results. However, we emphasize that there were no fitting parameters in our simulation to adjust the obtained results to the experimental data.

The rest of this paper is organized as follows. First, we outline the assumptions inherent in incorporating CNT to an MD simulation. The details for the calculation of the volumetric driving force necessary to link the MD simulation to higher-scale simulation are described. Next, we illustrate a new method for identifying precipitate phases. The full hybrid kMC/MD simulation procedure of precipitation is described, followed by joining the two methods together for the determination of the interface free energy. A final discussion of the scientifically relevant findings follows along with an outline of the primary conclusions and relevance to future efforts in materials development.

II. SIMULATION PROCEDURE

A. Main assumptions

The seeding method is based on the CNT equation relating the interface free energy, σ , to the change in the free energy associated with the formation of the critical nucleus, ΔG^* ,

$$\sigma = \frac{3}{2s} |\Delta \mu| \rho^{2/3} N^{*1/3},\tag{1}$$

where $\Delta\mu$ is the change in the bulk free energy associated with the phase transformation, ρ is the atomic density, N^* is the number of atoms in the critical nucleus, and s is the shape factor equal to the ratio of the nucleus area to its volume in the power of 2/3. We note that Eq. (1) is derived in the assumption that the shape factor does not depend on N, which is weaker than the assumption about the spherical nucleus shape. We also note that the same assumption leads to the following expression for the nucleation rate:

$$J = J_0 e^{-|\Delta \mu| N^* / 2k_B T}, \tag{2}$$

where J_0 is the kinetic prefactor and k_BT is the thermal factor. We note that this kinetic prefactor, J_0 , is needed to determine the nucleation rate from Eq. (2). However, it is not needed to determine the critical nucleus size, N*, because by definition the critical nucleus size is determined at J = 0. The interface free energy is not present in Eq. (2) and, hence, is not needed to get the nucleation rate. A derivation of this equation can be found from Sun et al. 10 Instead, determination of the nucleation rate requires only the critical nucleus size, N^* , which can be obtained from an atomistic simulation. The interface free energy can then be calculated from the value of N^* using Eq. (1), assuming that the shape factor is close to that of a sphere.

B. Volumetric driving force

Another quantity needed to obtain the nucleation rate is $\Delta \mu$. In principle, it can also be obtained through atomistic simulations. However, unlike the interface free energy, this quantity can be relatively easily and reliably obtained experimentally using the CALPHAD approach. In the present study, we used CALPHAD and KWN modeling inside of the Kawin software package. 16 Thermodynamic data for describing the Ni-Al phase behavior were taken from DFT-derived database information for the Al-Co-Cr-Ni system. 17 At 1000 K and 13% Al, the change in bulk free energy associated with the precipitation of Ni₃Al was calculated to be 205.10 J/mol, or 29.94 MJ/m^3 .

C. Precipitate phase identification

To measure the change in the size of the precipitates during nucleation and growth, the matrix and precipitate phases must be clearly distinguished. In the case of Ni-rich Ni-Al alloys, we needed an algorithm that would distinguish between the Al solution in the fcc Ni and the L₁₂ phase. Note that the underlying crystalline lattice of the L₁₂ phase is also fcc, but unlike the γ phase, the L₁₂ phase contains two sublattices: the Ni sublattice and the Al sublattice. An additional complexity comes from the fact that, when in contact with a Ni-rich γ phase at T = 1000 K, the equilibrium composition of the y' phase is 24.7% Al (for the employed semiempirical potential¹⁸) such that some Ni atoms reside on the Al sublattice.

As a test bed, we created a simulation cell containing 256 000 Ni atoms occupying an fcc lattice. Next, 13.5% of Ni atoms were substituted by Al atoms. A concentration of 13.5% was chosen as an initial starting point to provide a small driving force for precipitation with ~1% excess Al in the matrix phase. Finally, we inserted L₁₂ spheres with radii ranging from 7 to 17 Å in the center of the simulation cell (see Fig. 1). First, we tested the polyhedral template matching method incorporated into the OVITO package.¹⁵ Figure 1(b) shows that this method identifies too many small regions of L₁₂, because it only considers the arrangement of the first nearest neighbors for structural identification. An examination of Fig. 1 also shows that this identification algorithm systematically underestimates the nucleus sizes, because the Ni atoms on the interface are always assigned to the γ phase.

To improve the identification of the L₁₂ precipitates, we developed a method that considers the concentration of species in a range of neighbor shells. For each neighbor shell, the local concentration of atoms in that shell is considered and matched to a target range. If values lie within the accepted range, the central particle is assigned the appropriate phase identifier. The identification of γ' L₁₂ was conducted by first considering the Al atoms. The first neighbor shell (within 3 Å) was required to have no more than one Al atom, while the second neighbor shell (from 3 to 4 Å) was required to have 3 or more Al atoms, which is 50% of the equilibrium phase composition in fully periodic L₁₂. The third neighbor shell (from 4 to 4.63 Å) was restricted to have no more than two Al atoms, and the fourth neighbor shell (from 4.63 to 5.27 Å) was required to have more than three Al atoms. Setting a reduced number of Al atoms in the second and fourth shells and non-zero numbers of Al atoms in the first and third shells allows for identifying Al atoms on the "surface" of an L₁₂ precipitate. The cutoff numbers of Al atoms in each shell were chosen to fit to the known precipitate behavior as demonstrated in Fig. 2 (see the supplementary material for additional details). After the precipitate Al atoms were identified, Ni atoms were selected based on the number of Al precipitate atoms in their neighbor shells. The first neighbor shell was required to have two or more Al precipitate neighbors, and the second neighbor shell was required to have no Al precipitate atoms. The third neighbor shell could have any number of Al precipitate atoms, and the fourth shell was required to have no

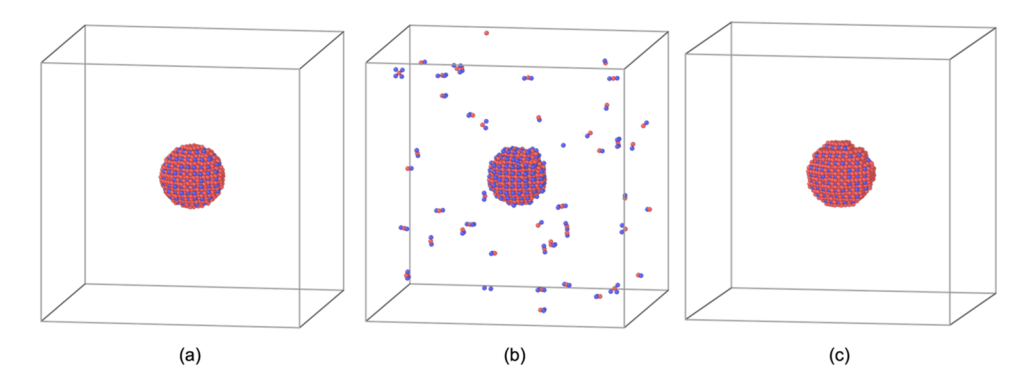


FIG. 1. Comparison of different precipitate identification methods. Panel (a) shows atoms belonging to the inserted L₁₂ precipitate. Panel (b) shows atoms that were identified as the L₁₂ atoms by the polyhedral template matching method (implemented in OVITO) removing single-atom clusters. Panel (c) shows atoms that were identified as the L₁₂ atoms by the neighbor shell concentration method developed in the present study. Ni atoms are shown in red, and Al atoms are shown in blue. Visualized by OVITO.15

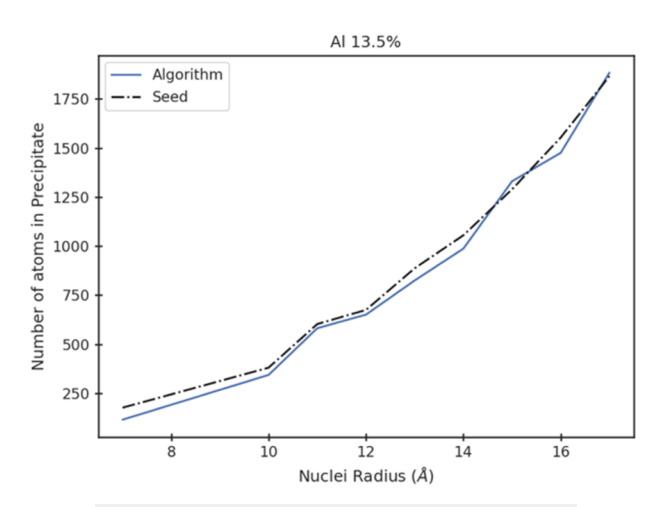


FIG. 2. Number of atoms assigned to initial L_{12} precipitates.

Al precipitate atoms. Figure 1(c) demonstrates a clear improvement in phase identification capability by the implementation of the new algorithm. Not only does our algorithm reduce the extraneous sites identified by the PTM, but it also properly identifies the Ni atoms close to the precipitate, which should be considered part of the L_{12} phase. This assists in more accurate calculation of the number of total precipitate atoms, especially for smaller precipitate sizes.

D. kMC/MD simulation

The simulation cell contained $40 \times 40 \times 40$ fcc unit cells. As constructed, the simulation cell contained only Ni atoms. Next, the Al atoms were randomly introduced by the substitution of the Ni atoms such that the Al concentration was equal to a preset value. The simulation cell was then divided into the main part (matrix) and source/sink region as shown in Fig. 3. The Al concentration in the source/sink region was kept constant during the kMC/MD simulation to provide a constant bulk driving force, discussed below. Finally, a central spherical precipitate region was initialized with Al atoms in an L_{12} configuration to form the initial γ' precipitate (see Fig. 3).

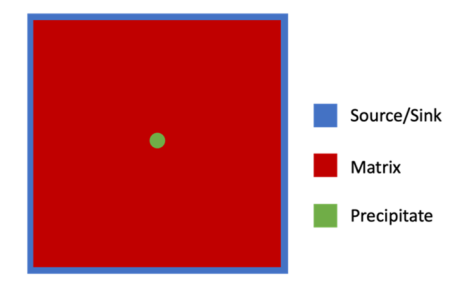


FIG. 3. Depiction of the simulation setup for constant-driving force precipitation. The outer region (blue) indicates a source/sink where concentration is held fixed surrounding an inner matrix region (red) of a supersaturated solid solution and a central precipitate seed (green).

All kMC/MD simulations were performed using LAMMPS. The MD simulation was performed using the NPT ensemble set to T = 1000 K and zero pressure, with fully periodic boundary conditions and a time step of 2 fs. The kMC algorithm attempted MC swaps of 1% Al atoms every 50 MD steps. These parameters affect the kinetics of the precipitate growth/shrinking, but their choice should not affect the interface free energy, which was the goal of the present atomistic study. Therefore, this choice of parameters was simply related to getting a maximum effective diffusion rate while maintaining acceptable MD conditions. This choice allowed us to get the largest amount of precipitate size change in the shortest amount of simulated MD time. The MC temperature was set equal to the thermostat temperature.

To provide a constant driving force of Al atoms, the number of Al atoms in the source/sink region was adjusted every 50 000 time steps. If the current concentration of the Al atoms in the matrix was lower than the preset concentration, Al atoms were added into the source/sink region by turning a given number of randomly chosen Ni atoms into Al atoms by the following equation:

$$N_{sw} = N_{ss}(X_0 - X), \tag{3}$$

where N_{sw} is the number of atoms to be swapped, N_{ss} is the number of total atoms in the source/sink region, X_0 is the target concentration, and X is the current concentration of Al atoms in the sink. If the concentration of Al atoms was higher than the preset concentration, Al atoms were removed by the reverse procedure.

E. Calculation of interface free energy

The critical nucleus size was determined by tracking the change in the precipitate size for initial precipitates of multiple sizes. The initial testing was conducted at 1000 K with an Al matrix concentration of 13.5%, providing an excess Al concentration of ~1% (see Fig. 4). Under these conditions, the initial precipitates always

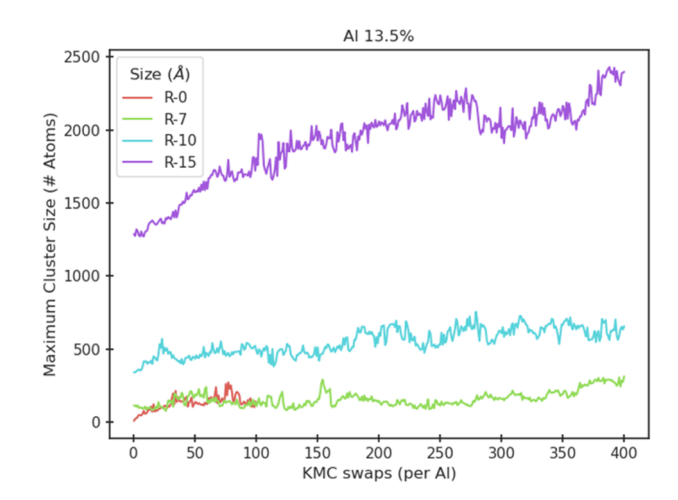


FIG. 4. Number of atoms in the largest precipitate vs number of KMC swaps attempted per Al atom for a Ni₃Al precipitate in an Ni–Al matrix with 13.5% Al. The colors indicate different initial precipitate radii in angstroms. A radius of 0 is for no seeded precipitate.

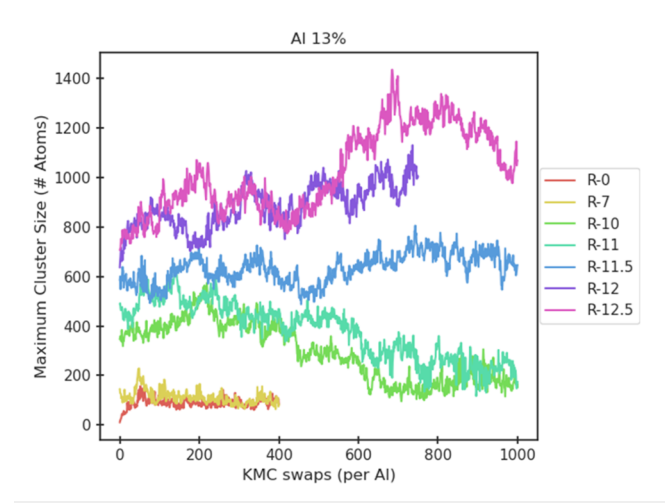


FIG. 5. Number of atoms in the largest precipitate vs number of KMC swaps attempted per Al atom for a Ni_3Al precipitate in an Ni_4Al matrix with 13% Al. The colors indicate different initial precipitate radii in angstroms. A radius of 0 is for no seeded precipitate.

grew even when its radius was 7 Å, which is the smallest possible nucleus size that can be identified due to the non-continuous nature of atomic arrangements. To verify these results, a simulation was conducted with no initial precipitate. Simulations with an initial precipitate of 7 Å and with no initial precipitate grew in the same manner when considering a matrix composition of 13.5% Al, with the 7 Å initial precipitate shrinking and being replaced by precipitates growing independently out of the matrix. Figure 4 demonstrates that the precipitate growth in this system mirrored the growth seen in the system with the 7 Å initial precipitate. Because

precipitates under 7 $\hbox{Å}$ grew, the critical nucleus size for these conditions must be less than 7 $\hbox{Å}$ and thus cannot be measured in our simulation.

To reduce the driving force for the precipitation and increase the corresponding critical radius size, we set up the Al concentration in the matrix to be 13%. This allowed for precipitates of small but measurable sizes to shrink, while larger precipitates grew (see Fig. 5). Nuclei with initial radii between 10 and 12 Å exhibited little change in precipitate size before subsequent growth or shrinkage for the first 400 KMC swaps per Al. This is a characteristic of precipitates near the critical nucleus size. Averaging the nuclei sizes over this range gave a critical nucleus size of 587 atoms. The variance in critical nuclei size is partially due to the discrete nature of the ordered γ' precipitate. To have distinctly different precipitate nuclei, a new plane of L₁₂ containing Al atoms must be added to the initial structure. If the external plane only contains Ni atoms, there is no discernible difference in the precipitate size between slightly larger and smaller precipitates. Likewise, once the 10 and 11 Å precipitates shrink, new precipitates with sizes <200 atoms similar to the 0 and 7 Å simulations are present in the system at a given snapshot, although the individual lifetime of such precipitates is short, since these precipitates are subcritical. The large difference in size between these subcritical nuclei and the critical nucleus size demonstrates the necessity of seeding the simulation with an initial precipitate.

Having identified a critical nucleus size, we determine the interfacial free energy for the system using Eq. (1) by incorporating a volumetric driving force calculated from CALPHAD. The resulting interfacial energy value is $17.4~\text{mJ/m}^2$ at 1000~K and a matrix composition of 13% Al.

The analysis of experimental results performed by Ardel ¹⁹ give an interface free energy value of 18.2 ± 3.5 mJ/m². Thus, our value is within 5% of this experimental value and well within the reported error.

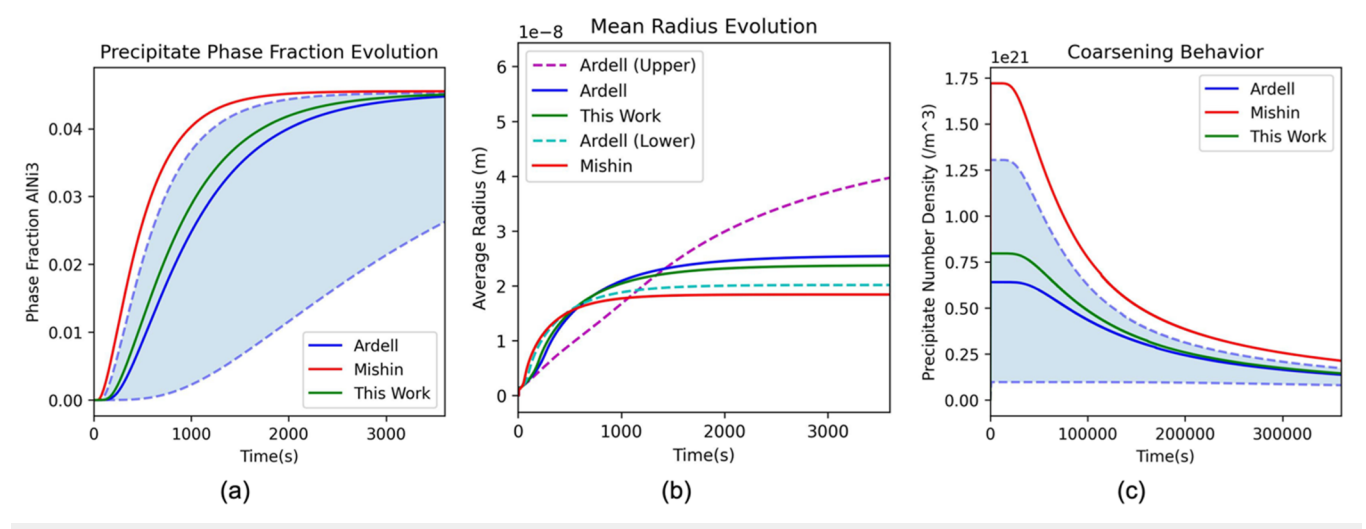


FIG. 6. Evolution of phase fraction (a), average radius (b), and precipitate number density (c) for 13% Al treated at 1000 K. The blue shaded regions indicate the standard deviation bounds for experimental values from Ardell. The values used for interfacial energy are 12.0 mJ/m² (Mishin⁴), 18.2 ± 3.5 mJ/m² (Ardell¹9), and 17.4 mJ/m² (this work)

III. DISCUSSION

In the earlier work by Mishin,⁴ the interfacial free energy of the Ni–Al γ/γ' interface along the (100) interface was determined using the CFM. To efficiently equilibrate the solid–solid system at a range of temperatures, a Monte Carlo approach was used. This approach resulted in an interfacial energy value to be 12.9 mJ/m² at T = 1000 K, which is 34% smaller than the experimental value. Our value is significantly closer to the experimental value. There can be several reasons for this improvement. First, the semiempirical potential employed in the present study much better reproduces the element partitioning between the γ and γ' phases than the potential employed in Ref. 4. Second, the CFM gives the stiffness value rather than the interface free energy itself. To get the interface free energy, it was assumed in Ref. 4 that its second derivative is negligible, which is not well justified.

To illustrate the significant impact that even small variations in interface energy can have on precipitation modeling, a series of KWN simulations were performed using Kawin using a range of interfacial energy values from this work and the literature. A 100 h heat treatment of a 13% Al sample at 1000 K was modeled using this work's calculated interface energy of 17.4 mJ/m², the interface energy obtained by Mishin⁴ (12.0 mJ/m²), and the temperature dependent interface energy (18.2 \pm 3.5 mJ/m²) obtained by Ardell. ¹⁹ The results of these simulations can be seen in Fig. 6. It is immediately apparent that even values within the range of the error bar provided by Ardell can have a massive impact on the predicted precipitation behavior, with energies at the upper and lower ends of the range at times resulting in a 10× increase in precipitate quantity or 4× increase in precipitate phase fraction. Our value is close enough to Ardell's that the precipitation behavior is mostly mirrored, but still at times exhibits meaningful differences, particularly in precipitate number density and matrix composition. For some applications, a difference of 0.1% concentration or a 30% increase in the number of precipitates would have a significant impact.

This highlights two issues endemic to precipitation modeling: that even a minor uncertainty in interface energy can have significant impacts on the precipitation behavior, and that minor changes in physical properties (that are themselves hard to measure) can result in very different calculated interface energies. By offering a means to calculate interface energies directly from atomic potentials, our method sidesteps both issues, allowing for an accurate interface energy to be obtained.

IV. CONCLUSIONS

An accurate calculation of critical nucleus size has been demonstrated using the hybrid kMC/MD simulation. Using this new approach, critical nuclei sizes can be determined more readily for systems of interest, provided that an accurate interatomic potential is available. When combined with CALPHAD predictions of the volumetric free energy, the determination of interfacial free energy purely from computational models enables more accurate precipitation models to be developed in systems for which experimental data are not readily available. This is critical for key materials systems and manufacturing techniques where precipitation occurs too rapidly to be readily measured in experiment. Likewise, the use of computational models to evaluate changes in interfacial free energy provides

an invaluable tool for improving our understanding and prediction of precipitation behavior.

SUPPLEMENTARY MATERIAL

The supplementary material includes the details of the precipitate identification algorithm summarized by Fig. 2 in the main text. The supplementary material also contains a figure with the results of precipitation calculations at 1000 K and 14% excess Al in the FCC matrix.

ACKNOWLEDGMENTS

J.P.T., M.I.M., and J.W.L. acknowledge funding from the NASA Aeronautics Research Mission Directorate (ARMD) Transformational Tools and Technologies (TTT) Project. R.A. and R.N. wish to acknowledge funding from the NSF through Grant No. 2119103 (DMREF) as well as Texas A&M ASCEND/TPT Program. Part of this research was carried out at the Jet Propulsion Laboratory (JPL), California Institute of Technology, USA, under a contract with the National Aeronautics and Space Administration (Grant No. 80NM0018D0004).

This work was authored by the employees of KBR Wyle Services, LLC, under Contract No. 80ARC020D0010 with the National Aeronautics and Space Administration. The United States Government retains and the publisher, by accepting the article for publication, acknowledges that the United States Government retains a non-exclusive, paid-up, irrevocable, worldwide license to reproduce, prepare derivative works, distribute copies to the public, and perform publicly and display publicly, or allow others to do so, for United States Government purposes. All other rights are reserved by the copyright owner.

AUTHOR DECLARATIONS

Conflict of Interest

The authors have no conflicts to disclose.

Author Contributions

J.P.T. wrote the code, conducted the simulation tests, prepared and edited the manuscript. M.I.M. conceived the research formulation, guided evaluation of the code, and edited the manuscript. R.N. performed the KWN and CALPHAD simulations and edited the manuscript. R.O. and R.A. guided the incorporation of KWN and CALPHAD modeling. J.W.L. secured funding and provided management support.

Jacob P. Tavenner: Conceptualization (equal); Data curation (equal); Formal analysis (equal); Investigation (equal); Methodology (equal); Software (equal); Validation (equal); Visualization (equal); Writing – original draft (equal); Writing – review & editing (equal). Mikhail I. Mendelev: Conceptualization (equal); Formal analysis (equal); Methodology (equal); Project administration (equal); Supervision (equal); Validation (equal); Writing – review & editing (equal). Raymond Neuberger: Investigation (supporting); Validation (equal); Visualization (supporting); Writing – review &

editing (supporting). Raymundo Arroyave: Funding acquisition (supporting); Supervision (supporting). Richard Otis: Methodology (supporting); Supervision (supporting); Validation (supporting). John W. Lawson: Funding acquisition (lead); Project administration (equal); Resources (lead); Supervision (equal); Writing – review & editing (supporting).

DATA AVAILABILITY

Data and code supporting this work can be provided upon request from the authors.

REFERENCES

- ¹J. Herrnring, B. Sundman, P. Staron, and B. Klusemann, "Modeling precipitation kinetics for multi-phase and multi-component systems using particle size distributions via a moving grid technique," Acta Mater. **215**(8), 117053 (2021).
- ²J. J. Hoyt, M. Asta, and A. Karma, "Method for computing the anisotropy of the solid-liquid interfacial free energy," Phys. Rev. Lett. **86**(24), 5530–5533 (2001).
- ³S. M. Foiles and J. J. Hoyt, "Computation of grain boundary stiffness and mobility from boundary fluctuations," Acta Mater. **54**, 3351–3357 (2006).
- ⁴Y. Mishin, "Calculation of the γ/γ " interface free energy in the Ni–Al system by the capillary fluctuation method," Modell. Simul. Mater. Sci. Eng. **22**(4), 045001 (2014).
- ⁵J. Q. Broughton and G. H. Gilmer, "Molecular dynamics investigation of the crystal-fluid interface. VI. Excess surface free energies of crystal-liquid systems," J. Chem. Phys. **84**(10), 5759–5768 (1986).
- ⁶R. L. Davidchack and B. B. Laird, "Direct calculation of the hard-sphere crystal melt interfacial free energy," Phys. Rev. Lett. **85**(22), 4751 (2000).
- ⁷X. M. Bai and M. Li, "Test of classical nucleation theory via molecular-dynamics simulation," J. Chem. Phys. **122**(22), 224510 (2005).

- ⁸E. Sanz, C. Vega, J. R. Espinosa, R. Caballero-Bernal, J. L. F. Abascal, and C. Valeriani, "Homogeneous ice nucleation at moderate supercooling from molecular simulation," J. Am. Chem. Soc. **135**(40), 15008–15017 (2013).
- ⁹T. Mandal and R. G. Larson, "Nucleation of urea from aqueous solution: Structure, critical size, and rate," J. Chem. Phys. **146**(13), 134501 (2017).
- ¹⁰Y. Sun, H. Song, F. Zhang, L. Yang, Y. Zhou, M. I. Mendelev, C. Z. Wang, and K. M. Ho, "Overcoming the time limitation in molecular dynamics simulation of crystal nucleation: A persistent-embryo approach," Phys. Rev. Lett. 120(8), 085703 (2018).
- ¹¹J. P. Tavenner, M. I. Mendelev, and J. W. Lawson, "Molecular dynamics based kinetic Monte Carlo simulation for accelerated diffusion," Comput. Mater. Sci. **218**, 111929 (2023).
- ¹² A. P. Thompson, H. M. Aktulga, R. Berger, D. S. Bolintineanu, M. W. Brown, P. S. Crozier, P. J. Veld, A. Kohlmeyer, S. G. Moore, T. D. Nguyen, R. Shan, M. J. Stevens, J. Tranchida, C. Trott, and S. J. Plimpton, "LAMMPS A flexible simulation tool for particle-based materials modeling at the atomic, meso, and continuum scales," Comput. Phys. Commun. 271(2), 108171 (2022).
- 13 M. W. Finnis and J. E. Sinclair, "A simple empirical N-body potential for transition metals," Philos. Mag. A 50(1), 45–55 (1984).
- ¹⁴M. I. Mendelev, 2022–Mendelev-M-I–Ni-Al, 2022, available at https://www.ctcms.nist.gov/potentials/entry/2022–Mendelev-M-I–Ni-Al/.
- ¹⁵A. Stukowski, "Visualization and analysis of atomistic simulation data with OVITO-the Open Visualization Tool," Modell. Simul. Mater. Sci. Eng. 18(1), 015012 (2010).
- ¹⁶N. Ury, R. Neuberger, N. Sargent, W. Xiong, A. Raymundo, and R. Otis, "Kawin: An open source Kampmann–Wagner Numerical (KWN) phase precipitation and coarsening model," Acta Mater. 255, 118988 (2023).
- ¹⁷L. L. Xuan, G. Lindwall, T. Gheno, and Z.-K. Liu, "Thermodynamic modeling of Al-Co-Cr, Al-Co-Ni, Co-Cr-Ni ternary systems towards a description for Al-Co-Cr-Ni," Calphad **52**, 125-142 (2016).
- ¹⁸V. V. Borovikov, M. I. Mendelev, T. M. Smith, and J. W. Lawson, "Molecular dynamics simulation of twin nucleation and growth in Ni-based superalloys," Int. J. Plast. **166**, 103645 (2023).
- 19 A. J. Ardel, "Temperature dependence of the γ/γ' interfacial energy in binary Ni–Al alloys," Metall. Mater. Trans. A 52, 5182 (2021).